Society For Biomaterials

Evaluation of dehydrated human umbilical cord biological properties for wound care and soft tissue healing

Jenn D. Bullard,† Jennifer Lei,† Jeremy J. Lim, Michelle Massee, Anna M. Fallon, Thomas J. Koob

MiMedx Group, Inc., Marietta, Georgia 30062

Received 19 January 2018; revised 16 May 2018; accepted 27 June 2018
Published online 10 September 2018 in Wiley Online Library (wileyonlinelibrary.com). DOI: 10.1002/jbm.b.34196

Abstract: Chronic wounds are a significant health care problem with serious implications for quality of life because they do not properly heal and often require therapeutic intervention. Amniotic membrane allografts have been successfully used as a biologic therapy to promote soft tissue healing; however, the umbilical cord, another placental-derived tissue, has also recently garnered interest because of its unique composition but similar placental tissue origin. The aim of this study was to characterize PURION® PLUS Processed dehydrated human umbilical cord (dHUC) and evaluate the biological properties of this tissue that contribute to healing. This was performed through the characterization of the tissue composition, evaluation of *in vitro* cellular response to dHUC treatment, and *in vivo* bioresorption and tissue response in a rat model. It was observed that dHUC contains collagen I, hyaluronic acid, laminin, and fibronectin. Additionally, 461 proteins that consist of growth factors and cytokines, inflammatory modulators, chemokines, proteases and inhibitors, adhesion molecules, signaling receptors, membrane-bound proteins, and other soluble regulators were detected. Cell-based assays demonstrated an increase in adipose-derived stem cell and mesenchymal stem cell proliferation, fibroblast migration and endothelial progenitor cell vessel formation in a dose-dependent manner after dHUC treatment. Lastly, rat subcutaneous implantation demonstrated biocompatibility since dHUC allografts were resorbed without fibrous encapsulation. These findings establish that dHUC possesses biological properties that stimulate cellular responses important for soft tissue healing. © 2018 The Authors. Journal Of Biomedical Materials Research Part B: Applied Biomaterials Published By Wiley Periodicals, Inc. J Biomed Mater Res Part B: Appl Biomater 107B: 1035–1046, 2019.

Key Words: umbilical cord, wound healing, chronic wounds, dehydrated human umbilical cord, Wharton's jelly

How to cite this article: Bullard JD, Lei J, Lim JJ, Massee M, Fallon AM, Koob TJ. 2019. Evaluation of dehydrated human umbilical cord biological properties for wound care and soft tissue healing. J Biomed Mater Res Part B 2019:107B:1035–1046.

INTRODUCTION

Normal wound healing is a dynamic series of regulated interactions and cellular infiltrates that can be summarized as four high-level and sequential, yet overlapping phases: hemostasis, inflammation, cellular proliferation, and tissue remodeling.[1,2] The hemostasis phase occurs immediately after injury when a blood clot is formed and platelets release clotting factors and growth factors at the injury site.[3,4] Subsequently, neutrophils and macrophages enter the wound bed during the inflammatory phase to phagocytose damaged tissue, foreign materials, and bacteria.[4] During cellular proliferation, fibroblasts deposit new extracellular matrix (ECM), which is ultimately remodeled into an organized, crosslinked collagen matrix as the wound transitions into the final remodeling phase.

A more detailed perspective of each of these phases highlights the complex interaction between growth factors, cytokines, the ECM, and cells to drive the progression through the healing cascade. For example, during the inflammatory phase, recruited activated macrophages clear the wound bed, and secrete numerous growth factors such as vascular endothelial growth factor (VEGF) to initiate formation of vasculature and stimulates collagen deposition by fibroblasts,[5] marking the onset of the proliferative phase. Additionally, fibroblast growth factor-2 (FGF-2) binding to heparan sulfate proteoglycans to act as a mitogen and epidermal growth factor (EGF) receptors binding to laminin enhances fibroblast migration.[6] During the remodeling phase, integrin-mediated cell binding and growth factors can regulate angiogenesis and the production and degradation of the ECM.[7,8] Upon successful resolution, the wound tissue resembles that of normal uninjured tissue, and cell signaling returns to homeostasis. In a chronic wound environment, typically caused by systemic abnormalities such as diabetes or venous insufficiency, the healing process may be stalled due to dysregulation of cytokine signaling, and elevated protease activity.[9,10] As a result, chronic wounds do not resolve properly resulting in the need for therapeutic intervention to promote closure of the wound.

Additional Supporting Information may be found in the online version of this article.
†These authors contributed equally to this work.
This is an open access article under the terms of the Creative Commons Attribution-NonCommercial-NoDerivs License, which permits use and distribution in any medium, provided the original work is properly cited, the use is non-commercial and no modifications or adaptations are made.
Correspondence: J. Lei; e-mail: jlei@mimedx.com
Contract grant sponsor: MiMedx Group, Inc.

Fetal chorioamniotic membranes are widely accepted as a therapeutic option for the healing of cutaneous wounds due to their immunologically privileged status and bioactive properties.[11–13] Although these fetal membranes have been successfully used for the treatment of chronic wounds,[14,15] the umbilical cord has garnered increasing attention as an allograft for soft tissue healing.[16–19] The umbilical cord transports oxygen and nutrients from the placenta to the fetus during gestation and is composed of amnion epithelium, two arteries, one vein, and Wharton's jelly.[20] Wharton's jelly is a collagenous matrix within the umbilical cord that protects the umbilical vessels and contains an abundance of hyaluronic acid (HA).[20] Much research has focused on the cells isolated from umbilical tissue as well as umbilical cord blood; however, the cord itself has not been well characterized. For example, mesenchymal stem cells (MSCs) derived from cord blood and Wharton's jelly are reported to be immunologically privileged and contain anti-fibrotic characteristics that may promote scarless wound healing.[21–23] Preliminary studies have shown that a cryopreserved umbilical cord product has been used as a graft to treat complex foot ulcers and can promote re-epithelialization in a murine corneal abrasion model,[24,25] indicating that the tissue of the umbilical cord has therapeutic potential in promoting soft tissue healing. However, it has yet to be determined whether these properties and biological signals also exist in a dehydrated form of the umbilical cord matrix as well.

The aim of this study was to characterize PURION® PLUS-Processed dehydrated human umbilical cord (dHUC) and identify its biological properties relevant to wound healing. This was performed by characterizing the composition of the tissue, evaluating *in vitro* cellular responses, including, stem cell proliferation, fibroblast migration, and angiogenic potential of endothelial cells, and assessing *in vivo* biocompatibility and resorption in a rat subcutaneous implantation model. PURION® PLUS Processed umbilical cord tissue (dHUC, EpiCord, MiMedx Group, Inc.) is processed using a similar technology to PURION® Processed dehydrated human amnion chorion membrane (dHACM; EpiFix/AmnioFix, MiMedx Group, Inc.).[11–13] Previous studies have demonstrated that this proprietary process results in an amniotic allograft with retained biological activity, which promotes accelerated wound closure of diabetic foot ulcers and venous leg ulcers when compared with standard treatments.[26–28] The novel umbilical cord tissue, dHUC, is believed to also be a promising treatment option for healing wounds and soft tissue injuries.

METHODS AND MATERIALS

Umbilical cord allografts

Human placentas were donated under informed consent following Caesarean section births, in compliance with the Food and Drug Administration's (FDA) Good Tissue Practice and American Association of Tissue Banks (AATB) standards. All donors were tested and confirmed free of infectious diseases, including human immunodeficiency virus (HIV), human T-lymphotrophic virus (HTLV), hepatitis B and C, and syphilis.

Umbilical cords were detached from the placenta, and the vein and arteries were removed. The resultant tissue was gently cleansed with the proprietary PURION® PLUS Process, then lyophilized and terminally sterilized by electron-beam irradiation (17.5–30 kGy). The PURION® PLUS Process is fundamentally similar to the patented PURION® Process; however, slight modifications have been optimized for umbilical cord tissue. A detailed disclosure of the general cleansing and decontamination steps that are applied to MiMedx's placental tissue-based products is provided in the specification of U.S. Patent No. 8,709,494. A sheet configuration of dHUC (EpiCord®, MiMedx Group, Inc.) was used as the test material for this study.

Histology

The dHUC tissue (n = 1 donor) was rehydrated in normal saline for 10 min prior to embedding in TissueTek optimal cutting temperature (OCT) compound (Sakura Finetek). Embedded tissues were snap frozen and cryosectioned at 10 μm thickness. Sections were fixed by incubation in acetone for 10 min and dried at room temperature for a minimum of 30 min. The sections were washed with phosphate buffered saline (PBS), blocked in donkey serum (Abcam), and stained with mouse anti-human collagen type I and sheep anti-human hyaluronic acid primary antibodies (Abcam). Immunoreactivity was detected using fluorescently conjugated donkey anti-mouse IgG and donkey anti-sheep IgG secondary antibodies (Life Technologies). Cell nuclei were counterstained with DAPI, and sections were imaged under fluorescence microscopy.

Extracellular matrix composition

For HA measurements, dHUC samples (n = 6 donors) were prepared by extracting minced tissue at 20 mg/mL concentration in RIPA buffer (ThermoFisher) with gentle agitation overnight at 4°C. Following a 24 h extraction, samples were centrifuged and passed through a 0.22 μm filter to remove residual tissue components. HA was quantified in each sample using a single factor enzyme-linked immunoabsorbent assay (ELISA, TECO) and calculated using HA standards provided by the kit, following the manufacturer's protocol.

For laminin and fibronectin measurements, dHUC samples (n = 6 donors) were extracted in 4 M guanidine hydrochloride and 0.1 M sodium acetate containing Protease Inhibitor Cocktail Set III (Calbiochem) overnight at 4°C and pH 6.0. Supernatants were collected and frozen at −20°C. Residual tissue was resuspended in a second volume of extraction buffer and processed identically. Supernatants from both extractions were combined and dialyzed using 50 kDa MWCO dialysis tubing (Spectrum) against deionized water for 2 days, and then frozen and lyophilized. Dried samples were reconstituted in PBS, and laminin and fibronectin content were measured using single-factor ELISAs (Abcam, R&D Systems). Laminin and fibronectin were quantified using standards provided by the kits, following the manufacturer's protocols.

Total soluble protein characterization

The dHUC samples (n = 5 donors) were minced, weighed and submitted to RayBiotech (Norcross, GA) for analysis. Upon receipt, tissue was incubated in lysis buffer (Raybiotech) containing protease inhibitor at an extraction concentration of 100 mg/mL with gentle agitation overnight at 4°C. Lysates were centrifuged, diluted with assay diluent and analyzed on a multiplex ELISA Quantibody® array (Q600 Human Cytokine Antibody Array, RayBiotech). The Quantibody array kit assays a total of 600 biomolecular analytes including cytokines, chemokines, receptors, matrix proteins, proteases, and protease inhibitors. System suitability positive controls consisted of samples of known concentration, and Quantibody® assay diluent was used as a negative control. Raw fluorescence data for each analyte was normalized against background fluorescence. Standard curves of known concentrations for each analyte, as provided by the array kit, were assayed and used to calculate quantities in each sample. Data were reviewed by MiMedx, and analyte content was calculated as picogram of analyte per milligram of dry tissue. Classifications of analytes were determined by the RayBiotech arrays used, literature review for the individual analytes, and the PANTHER classification system.[29]

Stem cell proliferation *in vitro*

To prepare soluble extracts of dHUC for cell culture experiments, sterilized grafts from individual donors were minced and extracted at 20 mg/mL overnight in basal medium (without serum) appropriate for the cell type evaluated (n = 10 donors). The tissue residue was removed by centrifugation and passage through a 0.22 μm filter. Extracts were then diluted in basal medium to the appropriate testing concentrations. Individual donors were used as separate treatments per well.

Normal adipose derived stem cells (ADSCs, Lonza PT-5006) and normal human bone marrow derived mesenchymal stem cells (MSCs, Lonza PT-2501) were plated on 96-well plates (Corning) at 2500 cells/well overnight in complete medium containing 10% fetal bovine serum (FBS, Lonza), 1% L-glutamine, and gentamicin-amphotericin B (Lonza). The following day, the medium was aspirated from the wells and washed with sterile PBS. The medium was replaced with the following treatments: basal medium without serum (negative control), complete medium with 10% FBS (positive control), and dHUC extracts at 20, 10, 5, and 1 mg/mL concentrations in basal medium. After 3 days in culture, the cells were washed with PBS, and a CyQUANT assay (Invitrogen) was performed to quantify DNA content as a measure of cellular proliferation following manufacturer's instruction. DNA content was translated to cell number, using a standard curve of known quantities of ADSCs or MSCs, respectively, as determined by counting on a hemocytometer.

Human dermal fibroblast migration *in vitro*

Adult human dermal fibroblasts (HDF, Gibco) were plated at confluence (10,000 cells/well) in a 96-well Image-Lock plate (Essen Bioscience) and serum-deprived overnight in medium containing 1% FBS. The following day, a standardized cell-free lane (scratch) was created in each well using a Wound-Maker tool (Essen Bioscience). The cell-free lanes were washed with basal medium to remove cell fragments and remaining serum and subsequently treated with one of the following: basal medium without serum (negative control), complete medium with 10% FBS (positive control), and dHUC extracts at 20 mg/mL in basal medium (n = 10 donors). Soluble dHUC extracts were prepared as previously described.

The plates were transferred to the IncuCyte ZOOM imaging system (Software Version 2016B; Essen Bioscience) and imaged every 6 h for a total of 72 h. Percent wound confluence was determined using an image processing algorithm to differentiate HDF cells and cellular debris from background to avoid the influence of user bias during image analysis.

Vessel formation studies using adipose-derived stem cells and endothelial colony forming cells *in vitro*

ADSCs and human endothelial colony forming cells (ECFCs, Essen Biosciences) provided in the Angiogenesis StemKit (Essen) were used to establish a co-culture in a 96-well plate according to the manufacturer's instructions. Briefly, the ECFCs, which are tagged with green fluorescent protein to allow fluorescent visualization of the tubule formation, were plated at 5750 cells/well on top of an ADSC monolayer that was plated at 40,000 cells/well. Once the co-culture was established, the cells were treated with the following: assay medium +20 ng/mL vascular endothelial growth factor (VEGF, positive control), assay medium +20 ng/mL VEGF +100 μm suramin (negative control), assay medium alone (vehicle control), and dHUC extracts at 10, 5, and 1 mg/mL concentrations in assay medium. The positive control was supplemented with the growth factor VEGF due to its known ability to induce angiogenesis and tubule formation and the negative control includes suramin, which is a compound that has proven anti-angiogenic properties. The dHUC extracts (n = 4 donors) were prepared as previously described.

The culture plate was placed into the IncuCyte system (Essen Biosciences) and imaged every 6 h for 72 h. Tube formation by the ECFCs was quantified as a measure of angiogenic potential. The network area (mm^2/mm^2), defined as the sum of the areas of all the networks in the image divided by the image area, and the network length (mm/mm^2), defined as the sum of the lengths of all the networks in the image divided by the image area, was determined using the Angiogenesis module in the IncuCyte software, which gives a quantitative scoring of tube formation.

Biocompatibility and bioresorption of dHUC *in vivo*

To examine biocompatibility and bioresorption of dHUC *in vivo*, 5 mm × 5 mm dHUC grafts were implanted subcutaneously in 22 normal, immune competent Sprague–Dawley rats (8-week-old, 12 male and 12 female) by Translational Testing and Training (T3) Laboratories (Atlanta, GA) and tracked for up to 97 days. Prior to the procedure, rats were housed two per cage of the same sex, and after the

TABLE I. Overall Inflammation Scoring

Score	Description
0	0, none.
1	Rare, 1–5/hpf
2	Mild, 5–10/hpf
3	Moderate, heavy infiltrate
4	Severe, packed

Hpf, high powered (400×) field.

procedure, animals were singly housed to prevent disruption of the implant site. Animals were anesthetized with isoflurane gas and placed in ventral recumbency. The dorsum was shaved and scrubbed in preparation for the implants using standard aseptic technique. A 5 mm × 5 mm test article was trimmed immediately prior to implantation in a sterile field. The skin of the spine was lifted and an incision made to create a subcutaneous pocket, and one test article was placed in the pocket. Care was taken to ensure that the material was flat. After placement, the pocket was closed with suture and/or staples. The implant site was marked with non-absorbable suture. Implants were not marked within the tissue as they can be identified histologically. Tissue samples were harvested en bloc from the implant site 24 h (n = 2, one male and one female), 7, 14, 22, 42, and 97 days (n = 4, two male and two female) after implantation. The tissues were fixed in 10% neutral buffered formalin, embedded in paraffin, sectioned, and stained with hematoxylin and eosin (H&E) and Movat's Pentachrome stain (Alizée Pathology). The specimens were analyzed histologically and scored by an independent, board-certified histopathologist for biocompatibility, and bioresorption (Alizée Pathology, Thurmont, MD). The scoring used for overall inflammation and residual material are seen in Tables I and II, respectively. The evaluating pathologist was blinded during the evaluation and scoring, and then unblinded to compile the report. This study was executed according to an Institutional Animal Care and Use Committee (IACUC) approved protocol.

Statistical analysis

For quantitative analysis, individual donors were run in duplicate for the following assays: HA, fibronectin, laminin ELISAs; and triplicate for the following assays: ADSC and MSC proliferation, HDF migration, and vessel formation co-culture. For soluble protein analysis, one sample from each donor was tested. Quantitative data was reported as mean ± standard deviation. A one-way ANOVA and Tukey's post hoc analysis with $p \leq 0.05$ was run to determine statistical differences among the mean values of each group. For HDF migration, a one-way ANOVA and Tukey's post hoc analysis with $p \leq 0.05$ was performed on mean wound closure at the final time point.

RESULTS

Histological assessment and ECM components of dHUC

The histological images of dHUC revealed a spongy tissue. Additionally, the dHUC tissue stained positively for both collagen type I (Figure 1A) and hyaluronic acid (Figure 1B), the two most abundant matrix components in umbilical cord tissue.[20] The images demonstrated an even distribution of these extracellular matrix components throughout the tissue (Figure 1D). Positive DAPI staining also shows that intact, cellular components are retained in dHUC (Figure 1C). In the dHUC tissue, ELISA assays determined that 444.6 ± 176.8 ng/mg fibronectin, 183.0 ± 48.3 pg/mg laminin were present after guanidine extraction, and 676.5 ± 54.9 μg/mg HA were present after RIPA buffer extraction (Table III).

Total growth factor content

The Q600 multiplex ELISA Quantibody® array was used to detect growth factors, cytokines, receptors, proteases and inhibitors, transmembrane proteins, and chemokines present in dHUC tissue. The assay detected a total of 461 biomolecules retained in dHUC (Figure 2, Supporting Information Table S1). About 107 of the 461 analytes measured were identified as growth factors and cytokines associated with normal physiological mechanisms inherent in remodeling and homeostasis, and contributed 18% of the total soluble protein concentration. Inflammatory modulators (55 of 461 analytes) accounted for 4% and chemokines (32 of 461 analytes) accounted for 3% of the total concentration. Matrix and cell–cell adhesion receptors (41 of 461 analytes) contributed 18%, while signaling receptors (119 of 461 analytes) contributed to 13% of the entire detected protein concentration. Membrane bound and transmembrane proteins (60 of 461 analytes) contributed to 11% of the total soluble proteins. Proteases and inhibitors (34 of 461 analytes), which included matrix, serine, and cysteine types, accounted for 5% of the total soluble protein content. Lastly, other soluble regulators (13 of 461 analytes) accounted for 28% of the total protein content. The full list of analytes detected is reported in Supporting Information Table S1.

Stem cell proliferation

Cell proliferation in response to positive and negative controls and dHUC extracts was tested on two relevant cell types for healing and repair, ADSCs, and MSCs.[22,30] The positive control is each cell type's respective medium with supplement and the negative control is basal medium. For the ADSCs, there was no statistical difference between the positive control (complete media) and the 20 mg/mL dHUC treatment (Figure 3A). Similarly with the MSCs, there was

TABLE II. Residual Material Scoring

Score	Description
0	None present.
1	Extensive bioresorption with less than one third of original amount of test or control material remaining.
2	Moderate bioresorption with between one-third and two-thirds of original amount of test or control material remaining.
3	Mild bioresorption with approximately two-thirds of original amount of test or control material remaining.
4	Little to no bioresorption of residual test or control material.

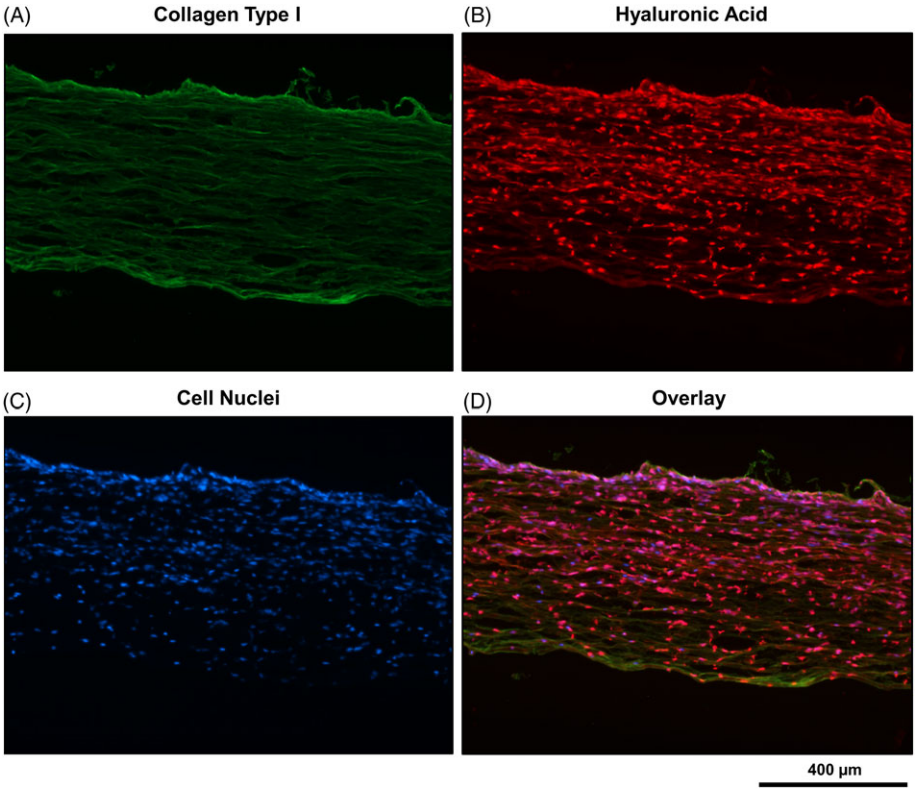

FIGURE 1. Immunofluorescence staining of dHUC grafts. (A) Type I collagen presence seen in green. (B) HA distribution in the tissue visible in red. (C) Cell nuclei are shown in blue. (D) The overlay shows the co-localization of hyaluronic acid (red) and cell nuclei (blue) in pink. Scale bar = 400 μm.

also no statistical difference between complete media, 20 and 10 mg/mL dHUC treatments (Figure 3B). The 20, 10, and 5 mg/mL concentrations of dHUC extracts promoted significantly more proliferation for both ADSCs and MSCs compared with the negative control (basal media). Additionally, the 1 mg/mL concentrations of dHUC did not result in significantly more proliferation compared with the negative control indicating dilution of the proliferative factors found in dHUC extracts. Phase images revealed that dHUC-treated ADSC and MSC morphology appeared like that of the positive control cells and confluence trended similar to cell number results (Figure 4). Overall, the dHUC extracts demonstrated a dose-dependent proliferative effect on both ADSCs and MSCs.

Fibroblast migration

Migration of HDFs into a scratch wound in response to 20 mg/mL dHUC extracts and controls was determined. Migration was assessed by tracking confluence of cells in the scratch area and reported as wound closure percentage, thus cell proliferation could also contribute to the wound closure. The positive control is medium supplemented with fetal bovine serum and the negative control is basal medium. After 72 h, dHUC extracts promoted significantly greater cell migration with an average of 78.5% ± 6.3% wound closure (Figure 5), compared with the negative control which sustained cell viability but stimulated a migratory response of only 43.9% ± 7.9% wound closure. The positive control, however, stimulated significantly greater HDF migration with a 97.2% ± 4.1% wound closure of the scratch compared with both the negative control and 20 mg/mL dHUC tissue extracts.

TABLE III. Extracellular Matrix Components Quantified in dHUC Tissue

ECM Component	Amount in dHUC
Fibronectin	444.6 ± 176.8 ng/mg
Laminin	183.0 ± 48.3 pg/mg
Hyaluronic acid	676.5 ± 54.9 μg/mg

Values are reported as average mass of matrix component per dry mass of tissue ± standard deviation.

Vessel formation

The effect of dHUC extracts and positive and negative controls on vessel formation within an ECFC and ADSC co-culture was examined as a measure of angiogenic potential over the course of 72 h (Figure 6). Over the first 24 h, both network length and area increased and plateaued around 32 h for the positive (assay media +20 ng/mL VEGF) and vehicle control (assay media only), and the dHUC treated groups. For the negative control (VEGF + Suramin) network length and area begin to decrease around 24 h after the initial increase (Figure 6A,C). At 72 h, network length and area by cells treated with the highest concentration of dHUC (10 mg/mL) were not significantly different from the positive control treatment (Figure 6B,D). The lower dose of dHUC (1 mg/mL) resulted in a significantly increased

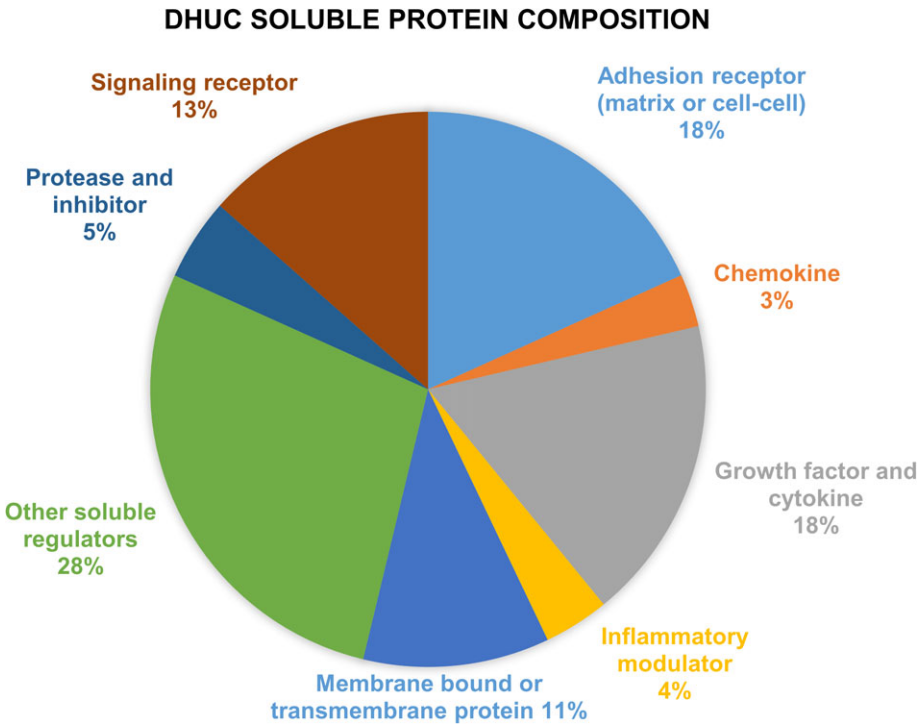

FIGURE 2. Protein composition of dehydrated human umbilical cord lysates. For each category, percentages reported represent the protein concentration (pg factor/mg tissue) normalized to the total protein amount detected.

network area and length compared with the negative control. In addition, 10 and 5 mg/mL dHUC treatment wells had significantly higher network areas and lengths compared with both the negative and the vehicle controls. A dose-dependent angiogenic response is evident with the 10, 5, and 1 mg/mL dHUC treatments. The fluorescent images taken with the IncuCyte show the established and refined network tubules promoted by the positive control and dHUC extract treatments after 72 h (Figure 7). The treatment with the addition of suramin (negative control), a known angiogenic inhibitor, contains little network or tubule branching from the ECFCs after 72 h as expected. These results show that dHUC extracts contain angiogenic factors that successfully promote *in vitro* vessel formation within this co-culture of ADSC and ECFC cells.

Biocompatibility and bioresorption of dHUC

Biocompatibility and bioresorption of dHUC allografts were determined *in vivo* in a subcutaneous rat model over 97 days following implantation, as scored by an independent, certified histopathologist. Histological images show continual tissue ingrowth into dHUC allografts, and dHUC underwent steady bioresorption with decreasing amounts of material present at the implant sites over time (Figure 8). The dHUC

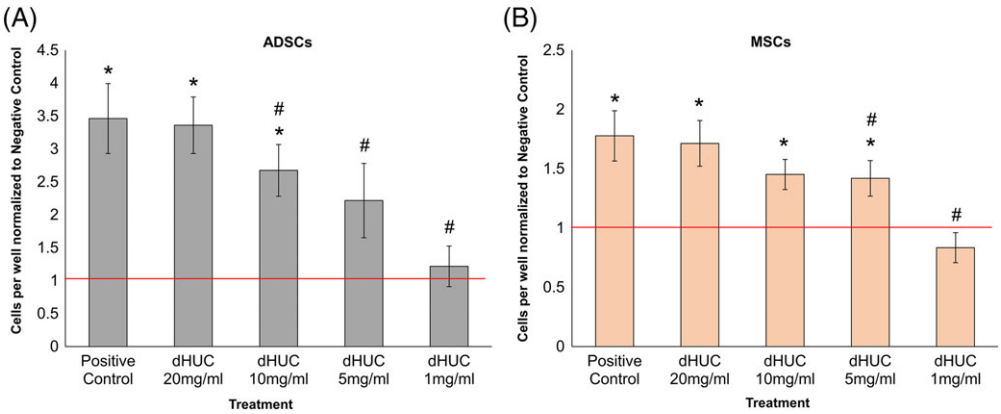

FIGURE 3. Proliferation of (A) ADSCs and (B) MSCs after 72 h in response to dHUC treatments. Bars represent the average number of cells per well normalized to the Negative Control (red line) ± standard deviation detected in each treatment and control wells. * indicates statistically significant difference from Negative Control; # indicates statistical difference from Positive Control; $p \leq 0.05$.

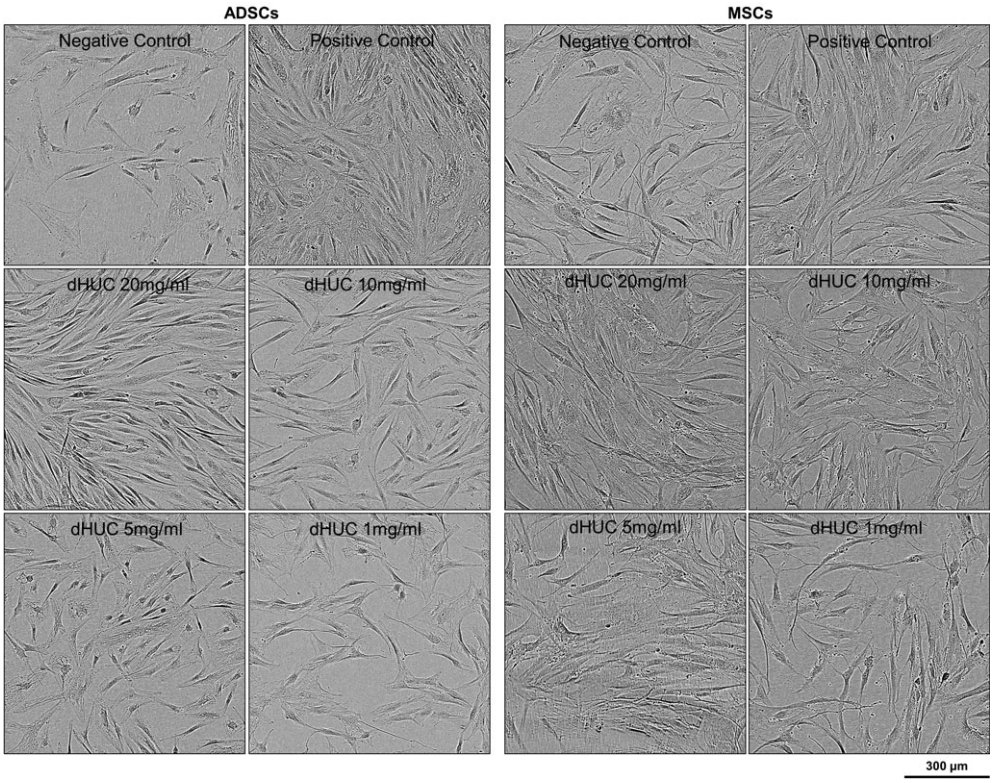

FIGURE 4. Phase images of (A) ADSCs and (B) MSCs at 72 h in response to control and dHUC treatments at 20, 10, 5, and 1 mg/mL. Scale bar = 300 µm.

was also biocompatible with minimal fibrous encapsulation observed after 97 days. Moderate inflammation was observed in dHUC implants after 42 days, however, inflammation declined after 97 days as the implant was degraded *in vivo* as shown by histologic scoring (Figure 9). At the 97 day time point dHUC was only detected in one of the four animals indicating substantial resorption in the other three animals.

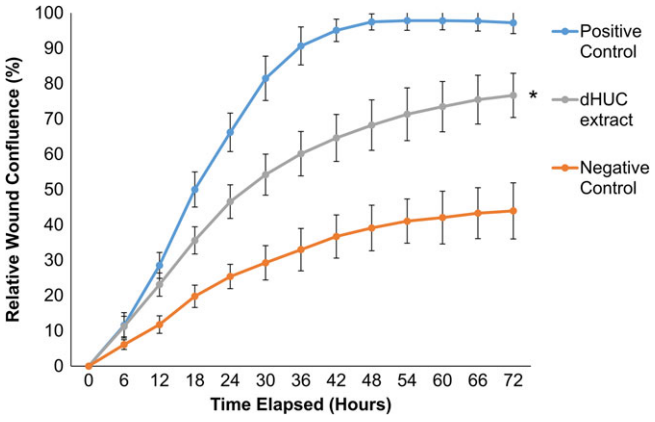

FIGURE 5. Migration of HDFs over 72 h in response to dHUC treatment (20 mg/mL) and Positive and Negative Controls. Values are reported as mean relative wound confluence (%) ± standard deviation. * indicates statistically significant difference from positive and negative controls at 72 h; $p \leq 0.05$.

DISCUSSION

This study characterized the biological properties of dHUC, evaluated the *in vitro* effects on proliferation, migration and angiogenesis, and determined its capacity to be resorbed in an *in vivo* rat subcutaneous implantation model. dHUC is a tissue that can be used as a wound covering to deliver components such as HA, a glycosaminoglycan that can retain water[31] and a myriad of bioactive factors to drive cellular activity.

Histological assessment revealed that the primary native ECM components found in the Wharton's jelly of umbilical cord tissue, collagen I and HA,[20] are retained in dHUC after processing (Figure 1). Because dHUC allografts are devitalized, cell nuclei are intact and still present in the tissue, as shown by DAPI staining. While there is growing concern for undesirable cellular debris in ECM-based scaffolds, the umbilical cord and other fetally derived placental tissues are immunological privileged tissues,[32] and there have been no reported adverse reactions attributed to the DNA or cell remnants in placental tissue allografts containing live or preserved devitalized cells.[15,27,33–35] Quantification of other ECM components, laminin and fibronectin, reveal that dHUC allografts contain proteins that are integral ECM biomolecules and that are involved in wound healing (Table III). Laminin has an essential role in tissue homeostasis and can regulate cell proliferation, differentiation, adhesion and migration.[36] Laminin-derived peptides have also recently been designed to improve tissue regeneration after injury due to their role in re-epithelialization and angiogenesis.[36]

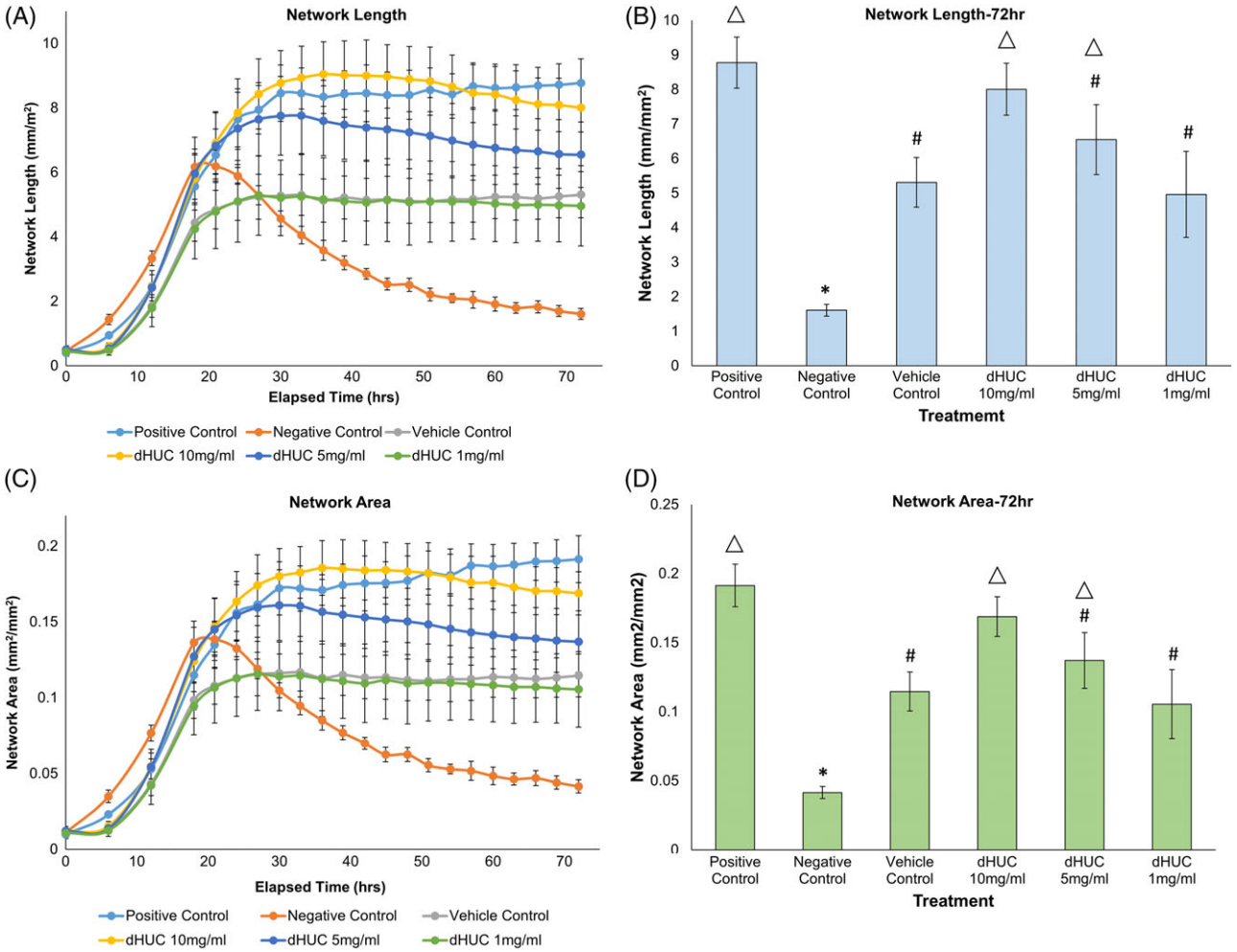

FIGURE 6. Angiogenic response from ECFCs after dHUC treatments. (A) Average network length (mm/mm^2) and (C) average network area (mm^2/mm^2) in response to dHUC extracts and controls over 72 h. (B) Network length and (D) network area at 72 h time point. Error bars represent the standard deviation from the mean values. * indicates statistical difference from all other groups; # indicates statistical difference from the positive control; Δ indicates statisical difference from the assay media only; $p \leq 0.05$.

The adhesion molecule, fibronectin, is found in the basement membrane of the ECM and is known to facilitate re-epithelialization during wound healing.[37] Overall, dHUC is proposed to be a tissue allograft that can provide an abundant matrix environment to augment healing in a variety of contexts.

About 461 protein biomolecules were detected in dHUC, with many of them being growth factors or cytokines that play a role in physiological processes involved in tissue remodeling and homeostasis (Figure 2). The full list of analytes measured can be found in Supporting Information Table S1. These include factors such as transforming growth factor-beta 1 (TGF-β1), platelet derived growth factor-AA (PDFG-AA), VEGF, and angiogenin-4, which are known to be involved in cell proliferation and angiogenesis.[3] Additionally, other detected factors include inflammatory modulators and chemokines, as well as proteases and inhibitors. Inflammatory modulators, such as interleukin-1 beta (IL-1β) and monocyte chemoattractant protein-1 (MCP-1), are known to stimulate macrophages and recruit neutrophils to an injury site.[38] The proteases and inhibitors detected include serine and cysteine proteases that can modify proteins to their active form, as well as matrix proteases and their inhibitors, such as matrix metalloproteinase-1 (MMP-1) and MMP-3 and tissue inhibitor of metalloproteinases (TIMPs)-1 and -2, that are important regulators of ECM turnover during the remodeling phase.[6] As reflected in the soluble protein analysis, dHUC is a biologically active tissue that contains many signaling factors capable of stimulating responses that occur during tissue regeneration. Similar factors have also been identified in dHACM, another placental-derived graft that has shown clinical efficacy in treatment of venous leg ulcers and refractory non-healing wounds.[11,26–28,34,39] Thus, it is believed that dHUC grafts have therapeutic potential to be effective in promoting closure of chronic wounds as well.

Another subset of factors identified were adhesion molecules, membrane bound cell receptor proteins, and signaling receptors. Adhesion molecules, such as vascular cell adhesion protein-1 (VCAM-1) and intercellular adhesion molecule-1 (ICAM-1), play important roles in facilitating the

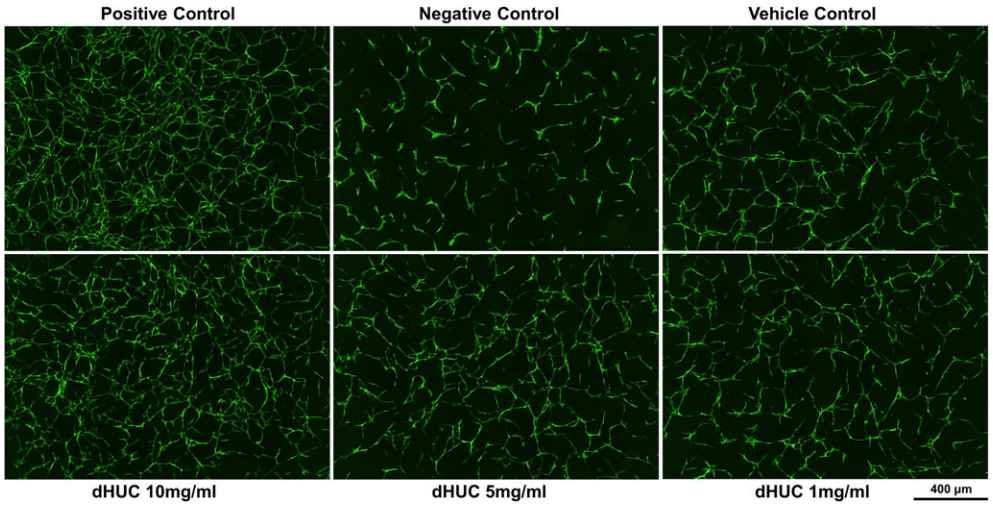

FIGURE 7. Fluorescent images of tagged endothelial cells (green) with positive, negative vehicle control treatments and dHUC treatments at 10, 5, and 1 mg/mL at 72 h. Scale bar = 500 µm.

cell-ECM and cell–cell interaction of neutrophils and macrophages during the inflammatory phase.[40] The receptors are typically present at the membrane surface of the cells and MSCs found within the umbilical cord.[41,42] The detection of these molecules indicate that the PURION® PLUS Process can help retain membrane bound factors natively present in umbilical cord despite the absence of viable cells after processing and lyophilization. Overall, dHUC is known to contain and retain a rich composition of factors that are involved in multiple phases of wound healing.

During the proliferation phase of wound healing, cells proliferate and secrete and deposit ECM to form new tissue.[3]

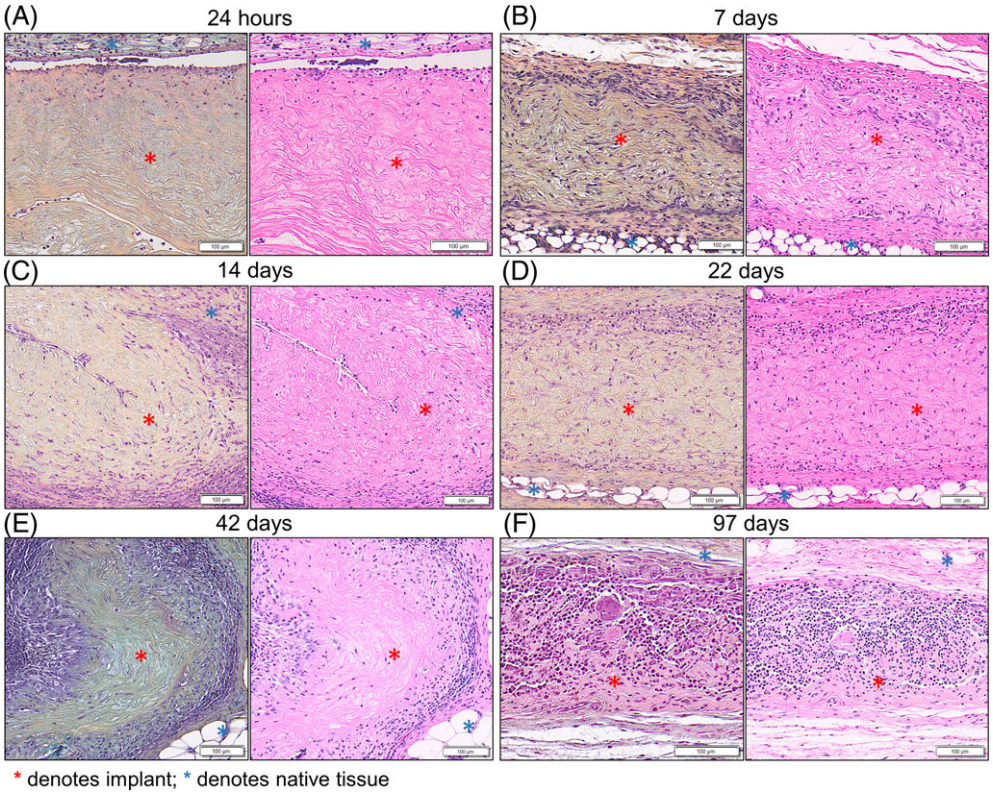

FIGURE 8. Biocompatibility and bioresorption of dHUC allografts in a rat subcutaneous implant model at (A) 24 h, (B) 7 days, (C) 14 days, (D) 22 days, (E) 42 days, and (F) 97 days. Images on the left were stained with Movat's Pentachrome (collagen is yellow, cell nuclei are black/purple, glycosaminoglycans are light blue, muscle and fibrin are red, and elastin is black) and images on the right were stained with hematoxylin and eosin. Scale bar = 100 µm.

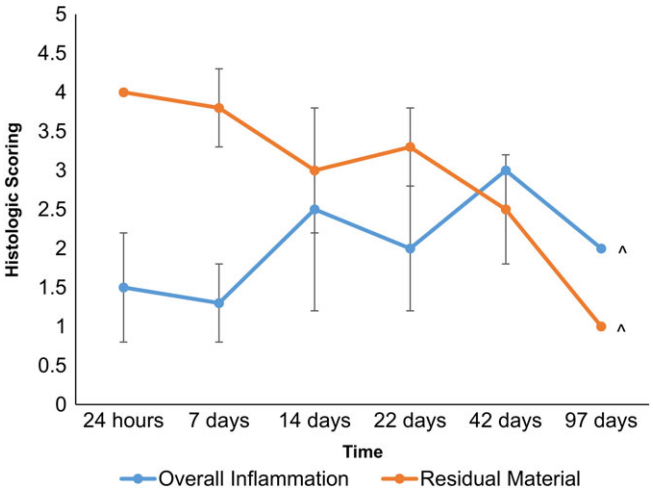

FIGURE 9. Histologic scoring for overall inflammation and residual implant material. Values reported as mean scoring ± standard deviation. ^ indicates scores that are only based on one sample because material could not be located in other animals.

In these studies, ADSC and MSCs were stimulated by dHUC extracts in a dose dependent manner to observe cell proliferation (Figures 3 and 4). In a deficient chronic wound environment, amplifying the presence and relative number of these cells could potentially supplement the healing cascade. ADSCs and MSCs are two types of stem cells that are capable of differentiating into different tissues[30,43] and have been shown to be involved in mediating homeostasis and tissue repair by secreting multiple growth factors which include, but are not limited to, hepatocyte growth factor (HGF), VEGF, TGF-β1, and basic FGF (bFGF).[44] Through paracrine signaling, these adult stem cells promote fibroblast collagen I secretion and fibroblast migration, and it has been shown that the delivery of ADSCs alone may result in significantly reduced wound size *in vivo*.[45] Also, MSCs derived from Wharton's jelly and umbilical cord blood have gained interest for transplantation as a cell therapy to repair damaged tissue in skin wound infections through paracrine effects and decreased inflammatory reaction.[46]

Similarly, dermal fibroblasts migration in healing wounds is critical to create new granulation tissue and provide a matrix for additional cells and blood vessels to grow.[4] It was observed that the soluble factors in dHUC extracts promoted human dermal fibroblast wound closure, thus representing significant biological activity within umbilical cord allografts to stimulate cellular responses (Figure 5). Combined, these *in vitro* results support a proposed mechanism for dHUC as a regenerative therapy by promoting the endogenous cells at the site of delivery to repair the injured tissue and induce a potent healing response.

In a wound bed, granulation tissue appears first along with branching capillaries and blood vessels.[47] The formation of new blood vessels, or angiogenesis, occurs from the tubule formation of endothelial colony forming cells and is necessary to carry oxygen and nutrients to the newly formed tissue.[47] The results from the *in vitro* angiogenesis co-culture model demonstrate that dHUC extracts increased new tubule formation of endothelial colony forming cells with increasing extract concentrations (Figures 6 and 7). Upon treatment of the ADSCs and ECFCs, cells differentiated into tubules to form stable networks within the first 48 h, which is demonstrated by the initial increase in network length and area. These networks are maintained for up to 96 h without additional treatment, as seen by the plateau after the first 24 h in culture. Suramin, a known inhibitor of bFGF,[48] inhibits vascular retention, therefore the initial increase of tube length and area observed was attributed to the addition of VEGF, and the lack of persistence of those vessels, and thus decrease in length and area, was caused by the inhibitor.[49,50] It is known that VEGF and bFGF play an integral role in the stimulation, differentiation and establishment of angiogeneic networks by endothelial cells.[51] The effect from dHUC treatment is further validated by the presence of those angiogenic factors, as well as others such as angiogenin-4 and angiopoietin, in the tissue as determined by the soluble protein analysis (Supporting Information Table S1).[47]

For successful wound closure, the applied graft is resorbed or degraded while the adjacent cells secrete ECM molecules such as collagen and fibronectin to form new tissue.[52]. Preliminary *in vivo* studies revealed that over the course of approximately 3 months, the dHUC graft was resorbed into the subcutaneous surrounding tissue without fibrous encapsulation and with moderate inflammation that decreased over time (Figures 8 and 9). This indicates that dHUC in a rat model did not undergo fibrous encapsulation or immune rejection when implanted, despite being a human-derived tissue with intact cells in a xenogeneic host. While these results are promising, further studies are needed to characterize the wound closure capacity of dHUC grafts *in vivo*.

The results of this study suggest that dHUC is a promising therapy for the treatment of acute and chronic wounds due to its vast growth factor and protein content, ECM components and ability to promote cell responses such as proliferation, migration and angiogenesis. Additionally, it has been characterized that dHUC tissue does not elicit an adverse effect and is actively resorbed when implanted in a rat model. To date, this is the first published characterization of a dehydrated form of umbilical cord tissue. These findings demonstrate that dHUC has biological properties that can promote basic cell activity involved not only in wound closure but also other general healing responses that can be found in soft tissues.

ACKNOWLEDGMENTS

JL, JDB, JJL, MM, AMF, TJK are employees of MiMedx Group, Inc. Growth factor multiplex ELISA arrays were performed by an independent CRO, RayBiotech, Inc. (Norcross, GA). Rat bioresorption study was performed by an independent CRO, T3 Labs (Atlanta, GA), with histopathology performed by Alizée Pathology (Thurmont, MD). The authors also thank Heather Bara PhD, for valuable comments on an earlier version of the manuscript.

REFERENCES

1. Eming SA, Martin P, Tomic-Canic M. Wound repair and regeneration: Mechanisms, signaling, and translation. Sci Transl Med 2014; 2:265.
2. Frykberg RG, Banks J. Challenges in the treatment of chronic wounds. Adv Wound Care 2015;4:560–582.
3. Barrientos S, Stojadinovic O, Golinko MS, Brem H, Tomic-Canic M. Growth factors and cytokines in wound healing. Wound Repair Regen 2008;16:585–601.
4. Diegelmann RF. Wound healing: An overview of acute, fibrotic and delayed healing. Front Biosci 2004;9:283.
5. Wu WK, Llewellyn OPC, Bates DO, Nicholson LB, Dick AD. IL-10 regulation of macrophage VEGF production is dependent on macrophage polarisation and hypoxia. Immunobiology 2010;215:796–803.
6. Schultz GS, Wysocki A. Interactions between extracellular matrix and growth factors in wound healing. Wound Repair Regen 2009; 17:153–162.
7. Roberts AB, Heine UI, Flanders KC, Sporn MB. Transforming growth factor-beta. Major role in regulation of extracellular matrix. Ann N Y Acad Sci 1990;580:225–232.
8. Senger DR, Claffey KP, Benes JE, Perruzzi CA, Sergiou AP, Detmar M. Angiogenesis promoted by vascular endothelial growth factor: Regulation through alpha1beta1 and alpha2beta1 integrins. Proc Natl Acad Sci U S A 1997;94:13612–13617.
9. Wysocki AB, Grinnell F. Fibronectin profiles in normal and chronic wound fluid. Lab Invest 1990;63:825–831.
10. Wysocki AB, Staiano-Coico L, Grinnell F. Wound fluid from chronic leg ulcers contains elevated levels of metalloproteinases MMP-2 and MMP-9. J Invest Dermatol 1993;101:64–68.
11. Koob TJ, Lim JJ, Massee M, Zabek N, Denoziere G. Properties of dehydrated human amnion/chorion composite grafts: Implications for wound repair and soft tissue regeneration. J Biomed Mater Res Part B 2014;102:1353–1362.
12. Massee M, Chinn K, Lei J, Lim JJ, Young CS, Koob TJ. Dehydrated human amnion/chorion membrane regulates stem cell activity *in vitro*. J Biomed Mater Res Part B 2015;104:1332–1342.
13. Massee M, Chinn K, Lim JJ, Godwin L, Young CS, Koob TJ. Type I and II diabetic adipose-derived stem cells respond to dehydrated human amnion/chorion membrane allograft treatment by increasing proliferation, migration, and altering cytokine secretion. Adv Wound Care 2016;5:43–54.
14. Forbes J, Fetterolf DE. Dehydrated amniotic membrane allografts for the treatment of chronic wounds: A case series. J Wound Care 2012;21:1–5.
15. Mermet I, Pottier N, Sainthillier JM, Malugani C, Cairey-Remonnay S, Maddens S, Riethmuller D, Tiberghien P, Humbert P, Aubin F. Use of amniotic membrane transplantation in the treatment of venous leg ulcers. Wound Repair Regen 2007;15:459–464.
16. Couture M. A single-center, retrospective study of cryopreserved umbilical cord for wound healing in patients suffering from chronic wounds of the foot and ankle. Wounds 2016;28:217–225.
17. Cheng AMS, Chua L, Casa V, Tseng SC. Morselized amniotic membrane tissue for refractory corneal epithelial defects in cicatricial ocular surface diseases. Transl Vis Sci Technol 2016;5:1–9.
18. Raines AL, Shih MS, Chua L, Su CW, Tseng SC, O'Connell J. Efficacy of particulate amniotic membrane and umbilical cord tissues in attenuating cartilage destruction in an osteoarthritis model. Tissue Eng Part A 2017;23:12–19.
19. Hanselman AE, Lalli TAJ, Santrock RD. Topical review: Use of fetal tissue in foot and ankle surgery. Foot Ankle Spec 2015;8:297–304.
20. Spurway J, Logan P, Pak S. The development, structure and blood flow within the umbilical cord with particular reference to the venous system. Aust J Ultrasound Med 2012;15:97–102.
21. Kamolz LP, Keck M, Kasper C. Wharton's jelly mesenchymal stem cells promote wound healing and tissue regeneration. Stem Cell Res Ther 2014;4:1–2.
22. Arno AI, Amini-Nik S, Blit PH, Al-Shehab M, Belo C, Herer E, Tien CH, Jeschke MG. Human Wharton's jelly mesenchymal stem cells promote skin wound healing through paracrine signaling. Stem Cell Res Ther 2014;5:1–13.
23. Doi H, Kitajima Y, Luo L, Yan C, Tateishi S, Ono Y, Urata Y, Goto S, Mori R, Masuzaki H, Shimokawa I, Hirano A, Li TS. Potency of umbilical cord blood- and Wharton's jelly-derived mesenchymal stem cells for scarless wound healing. Sci Rep 2016;6:18844.
24. Caputo WJ, Vaquero C, Monterosa A, Monterosa P, Johnson E, Beggs D, Fahoury GJ. A retrospective study of cryopreserved umbilical cord as an adjunctive therapy to promote the healing of chronic, complex foot ulcers with underlying osteomyelitis. Wound Repair Regen 2016;24:885–893.
25. Tighe S, Moein HR, Chua L, Cheng A, Hamrah P, Tseng SC. Topical cryopreserved amniotic membrane and umbilical cord eye drops promote re-epithelialization in a murine corneal abrasion model. Invest Ophthalmol Vis Sci 2017;58:1586–1593.
26. Serena TE, Yaakov R, DiMarco DT, Le LT, Taffe E, Donaldson M, Miller M. Dehydrated human amnion/chorion membrane treatment of venous leg ulcers: Correlation between 4-week and 24-week outcomes. J Wound Care 2015;24:530–534.
27. Serena TE, Carter MJ, Le LT, Sabo MJ, DiMarco DT. A multicenter, randomized, controlled clinical trial evaluating the use of dehydrated human amnion/chorion membrane allografts and multilayer compression therapy vs. multilayer compression therapy alone in the treatment of venous leg ulcers. Wound Repair Regen 2014;22:688–693.
28. Sheikh ES, Fetterolf DE. Use of dehydrated human amniotic membrane allografts to promote healing in patients with refractory non healing wounds. Int Wound J 2014;11:711–717.
29. Mi H, Anushya M, Casagrande JT, Thomas PD. Large-scale gene function analysis with the PANTHER classification system. Nat Protoc 2013;8:1551–1566.
30. Hassan WUI, Greiser U, Wang W. Role of adipose-derived stem cells in wound healing. Wound Repair Regen 2014;22:313–325.
31. Singh A, Li P, Beachley V, McDonnell P, Elisseeff JH. A hyaluronic acid-binding contact lens with enhanced water retention. Contact Lens Anterior Eye 2015;38:79–84.
32. Uckan D, Steele A, Cherry, Wang BY, Chamizo W, Koutsonikolis A, Gilbert-Barness E, Good RA. Trophoblasts express Fas ligand: A proposed mechanism for immune privilege in placenta and maternal invasion. Mol Hum Reprod 1997;3:655–662.
33. Azuara-Blanco A, Pillai C, Dua HS. Amniotic membrane transplantation for ocular surface reconstruction. Br J Opthalmol 1999;83:399–402.
34. Bianchi C, Cazzell S, Vayser D, Reyzelman AM, Dosluoglu H, Tovmassian G, EpiFix VLU Study Group. A multicentre randomised controlled trial evaluating the efficacy of dehydrated human amnion/chorion membrane (EpiFix(R)) allograft for the treatment of venous leg ulcers. Int Wound J 2017;15:114–122.
35. Mrugala A, Sui A, Plummer M, Altman I, Papineau E, Frandsen D, Hill D, Ennis WJ. Amniotic membrane is a potential regenerative option for chronic non-healing wounds: A report of five cases receiving dehydrated human amnion/chorion membrane allograft. Int Wound J 2016;13:485–492.
36. Iorio V, Troughton LD, Hamill KJ. Laminins: Roles and utility in wound repair. Adv Wound Care 2015;4:250–263.
37. Lenselink EA. Role of fibronectin in normal wound healing. Int Wound J 2015;12:313–316.
38. Koh TJ, DiPietro LA. Inflammation and wound healing: The role of the macrophage. Exp Rev Mol Med 2011;13:1–12.
39. Koob TJ, Lim JJ, Massee M, Zabek N, Rennert R, Gurtner G, Li WW. Angiogenic properties of dehydrated human amnion/chorin allografts: Therapeutic potential for soft tissue repair and regeneration. Vasc Cell 2014;6:1–10.
40. Mutsaers SE, Bishop JE, McGrouther G, Laurent GJ. Mechanisms of tissue repair: From wound healing to fibrosis. Int J Biochem Cell Biol 1997;29:5–17.
41. Akerman F, Lei ZM, Rao CV. Human umbilical cord and fetal membranes co-express leptin and its receptor genes. Gynecol Endocrinol 2002;16:299–306.
42. Kim DS, Kim JH, Lee JK, Choi SJ, Kim JS, Jeun SS, Oh W, Yang YS, Chang JW. Overexpression of CXC chemokine receptors is required for the superior glioma-tracking property of umbilical cord blood-derived mesenchymal stem cells. Stem Cells Dev 2009;18: 511–519.
43. Wu L, Chen L, Scott PG, Tredget EE. Mesenchymal stem cells enhance wound healing through differentiation and angiogenesis. Transl Clin Res 2007;25:2648–2659.
44. Tsuji W, Rubin P, Marra KG. Adipose-derived stem cells: Implications in tissue regeneration. World J Stem Cells 2014;6:312–321.

45. Kim WS, Park BS, Sung JH, Yang JM, Park SB, Kwak SJ, Park JS. Wound healing effect of adipose-derived stem cells: A critical role of secretory factors on human dermal fibroblasts. J Dermatol Sci 2007;48:15–24.
46. Malgieri A, Kantzari E, Patrizi MP, Gambardella S. Bone marrow and umbilical cord blood human mesenchymal stem cells: State of the art. Int J Clin Exp Med 2010;3:248–269.
47. Tonnesen MG, Feng X, Clark RA. Angiogenesis in wound healing. J Invest Dermatol Symp Proc 2000;5:40–46.
48. Danesi R, Del Bioanchi S, Soldani RC, La Rocca RV, Myers CE, Paparelli A, Del Tacca M. Suramin inhibits bFGF-induced endothelial cell prolifeartion and angiogenesis in the chick chorioallantoic membrane. Br J Cancer 1993;68:932–938.
49. Tomanek RJ, Lotun K, Clark EB, Suvarna PR, Hu N. VEGF and bFGF stimulate myocardial vascularization in embryonic chick. Am J Physiol 1998;274:H1620–H1626.
50. Tomanek RJ, Sandra A, Zheng W, Brock T, Bjercke RJ, Holifield JS. Vascular endothelial growth factor and basic fibroblast growth factor differentially modulate early postnatal coronary angiogenesis. Circ Res 2001;88:1135–1141.
51. Ferrara N, Kerbel RS. Angiogenesis as a therapeutic target. Nature 2005;438:967–974.
52. Metcalfe AD, Ferguson MWJ. Tissue engineering of replacement skin: The crossroads if biomaterials, wound healing, embryonic development, stem cells and regeneration. J R Soc Interface 2007;4:413–437.